Spectral Ratio Imaging Methods for Geological Remote Sensing from Aircraft and Satellites

by

Robert K. Vincent
Environmental Research Institute of Michigan

ABSTRACT

The author has identified the following significant results. An R_{54} spectral ratio image (radiance in ERTS MSS channel 5 divided by channel 4 radiance) was found to enhance contrast between hematite, an iron oxide, and other natural materials in ERTS frame E-1013-17294, over the Wind River Range of Wyoming. Hematite, occurring in this frame as Triassic red beds and red pyroclastics, is brightest in an R_{54} ratio image, whereas it is neither brightest nor darkest in any other ratio image or in any single channel ERTS image. Magnetite, another iron oxide, is one of the darkest materials in the scene in an R_{74} ratio image. Reflectance ratios from approximately 350 laboratory spectra of soils, minerals, rocks, and some natural vegetation support these results. [Ratio codes for these laboratory spectra are given in Report No. 193300-16-P, of NASA Contract NAS9-9784.] The hematite spectrum has a higher R_{54} ratio than approximately 90% of the 350 laboratory curves. Likewise, a magnetite spectrum has a lower R_{74} ratio than approximately 90% of the spectra. The laboratory spectra predict that limonite, a field term for iron oxides containing relatively large amounts of H_2O, should be almost as bright as hematite in an R_{54} ratio image, but should be darker than almost any other material in an R_{76} ratio image. This cannot be tested in the Wind River Range area, however, because there are no large known exposures of limonite. The ability to discriminate iron oxides from each other and from other natural materials may be important in remote geochemical prospecting for certain ore bodies, such as iron, nickel, or copper-bearing gossans. This paper also discusses the application of photogrammetric techniques to ratio images of ERTS and aircraft multispectral scanners, and compares ratio images to single channel scanner images and aerial photography.

Presented to the Management Utilization of Remote Sensing Data Conference, American Society of Photogrammetry; Sioux Falls, South Dakota, 31 October 1973

SPECTRAL RATIO IMAGING METHODS FOR GEOLOGICAL REMOTE SENSING FROM AIRCRAFT AND SATELLITES

Robert K. Vincent
Environmental Research Institute of Michigan
Ann Arbor, Michigan 48197

BIOGRAPHICAL SKETCH

Robert K. Vincent is an Associate Research Geophysicist at the Environmental Research Institute of Michigan in Ann Arbor, Michigan, where he has specialized in geological remote sensing during the past three years. He received a B.S. in physics and B.A. in mathematics from Louisiana Tech University, an M.S. in physics at the University of Maryland, and then became an Air Force officer for four years, serving all of his tour of duty at Air Force Cambridge Research Laboratories in Bedford, Massachusetts. Since coming to ERIM he has completed all requirements except one (thesis) for a Ph.D. in the University of Michigan's Dept. of Geology and Mineralogy and he expects to complete the final requirement by October, 1973. He has published approximately 20 papers and 10 technical reports and is a principle investigator on both ERTS and Skylab projects.

ABSTRACT

The production of ratio images from multispectral scanner data is described and several examples of ratio images from aircraft and ERTS data are given for visible, reflective infrared, and thermal infrared wavelengths. The application of photogrammetric techniques to ratio images, defined for this paper as ratio scannergrammetry, is considerably aided by the lesser dependence of ratio images on atmospheric and solar illumination variations, compared with single channel scanner imagery or aerial photos. Ratio scannergrammetry is further aided by the proportionality between ratios of a target deduced from ratio images and ratios of reflectances calculated from laboratory spectra of samples from the target area. Consequently, ratios calculated from laboratory data can be used to predict which ratios are best for discriminating a given rock or mineral, to predict what other rocks or minerals will be confused with it, and finally, to place ratio scannergrammetry on an absolute basis, within an estimated standard error on the order of 5% to 10%. Examples of relative agreement between laboratory data and ratio images are given for two iron oxides, hematite and magnetite. ~~Hematite is brightest in an ERTS $R_{\frac{5}{4}}$ ratio image, and magnetite is darkest~~ (except for water) in an $R_{\frac{7}{4}}$ ratio image. Ten geologic applications are suggested for ratio scannergrammetry including exploration for construction materials, mineral deposits, and ophiolites; mapping of small exposures of rock outcrops in vegetated terrain, soils, stratigraphy, volcanic ash flows, beaches, and sand dunes; assessment of the extent of known mineralogical resources; and monitoring of open pit mining operations.

INTRODUCTION

Aerial photography has long been a useful tool for geologists. Cameras and film are relatively inexpensive, spatial resolution is excellent, and the services of trained photogrammetrists are available for interpretation of the aerial photos. In contrast, multispectral scanners have a short history; scanner imagery has become widely regarded as a useful tool for geological remote sensing only since the advent of ERTS-1 in 1972, when the cost of data collection was substantially reduced.

Accordingly, few trained scientists and technicians are yet able to make full use of scanner data. Most of the geological investigations with ERTS multispectral scanner (MSS) data are structural studies to map new linear features, a feat which can perhaps be performed as well or better by space photographs. Although these studies are aided by the reduced need for mosaicing associated with scanner images, compared with photographs, such studies do not utilize two of the most important advantages of a scanner over a camera: greater spectral range (photographic films are limited to wavelengths shorter than about 0.9μm, whereas scanners can operate out to 14μm and longer) and ease of quantitative processing (radiances detected in each single scanner channel can be treated separately for every spatial resolution element in the scene). Lithologic or geochemical mapping can utilize these scanner advantages, however, because useful compositional information exists at wavelengths out to 14μm, and consistent geochemical mapping at different times and places requires that the signals detected for each spatial resolution element in the scene be corrected for atmospheric and illumination effects.

A spectral technique for geological remote sensing is being developed [1, 2, 3, 4] which is intended to be employed in two ways. The first use involves transforming multispectral scanner data into ratio images, which are amenable to photogrammetric techniques and are less sensitive to atmospheric or solar illumination effects than either single channel scanner images or aerial photos. In this paper, I will call the application of photogrammetric techniques to scanner imagery "scannergrammetry", and their application to ratio images from scanner data will be called "ratio scannergrammetry". The second use of the ratioing technique is the production of automatic recognition maps. Only the former case will be addressed in this paper. The latter will be discussed at the Fourth Annual Remote Sensing in Arid Lands Conference in Tucson, Arizona in November.

DESCRIPTION OF RATIO IMAGES

Multispectral scanner data is typically collected on magnetic tape such that the radiance detected in each spectral channel of the scanner can be retrieved for each point in the scanned scene. In the past many scanner images have been single channel images, i.e., bright to dark on the image corresponded to high to low radiance, respectively, detected in the wavelength region defined by a single spectral channel. Single channel images of the type routinely provided by NASA share one of the same serious drawbacks of aerial photography, namely the variable effects of atmosphere, solar illumination, and (in the case of thermal infrared data) temperature, both within the scene and between scenes displaced in time and space. These drawbacks, in fact, seem to be largely responsible for the limited usefulness of aerial photographs and single channel scanner images for absolute measurements of target reflectance. Color composites which linearly combine two or more single channel radiances also share these problems with atmospheric and solar illumination variations. The typical normalization process for color composites, such as making clouds white, can produce large inaccuracies in the radiance from darker materials in the scene. Such color composites are useful primarily in a non-quantitative sense, and can vary a great deal in appearance from one manufacturer to the next.

Ratio images are capable of suppressing some of these undesirable effects. The production of visible and reflective infrared ratio images from satellite and high altitude aircraft data begins with the approximate removal of the additive atmospheric terms, commonly called path radiance. For low altitude ($\lesssim$ 1.5 km) aircraft data, the additive

term is usually ignored. The radiance of the darkest object in the scene is subtracted from the radiance of all other points in the scene for each spectral channel. The remaining radiance in each channel is then approximately proportional to the target reflectance. However, multiplicative terms, including atmospheric transmittance, solar irradiance, electronic gain factors, and what I call a shadow factor (taken to be any spectrally independent suppressor of direct solar illumination within the instantaneous field of view, such as shadowing or sloping away from the sun) are still present. The remaining radiance (after dark object subtraction) in one spectral channel is divided by the remaining radiance in another spectral channel to produce a spectral ratio for each point in the scene. The ratio signal is therefore an electronic voltage that is approximately directly proportional to the ratio of reflectances of the target in these two spectral channels. However, the shadow factor has been removed by the ratio, since it is spectrally independent. The theory is given elsewhere [4].

The resulting ratio voltage is input to a light source which is scanned in front of a moving film strip. A high voltage, corresponding to a large ratio, produces a bright spot on the filmstrip, and a low voltage produces a dark spot. When the ratio image is completed, a gray scale is produced which approximately calibrates the relationship between ratio voltage and film density. In other words, the ratio image is produced in a manner similar to a single channel scanner image, except that a voltage proportional to a ratio of target reflectances in two spectral regions is produced.

If there is one area in the scene for which the spectral reflectance is known, it is possible to determine the proportionality constant between the ratio voltage for a given pair of spectral channels and the actual ratio of spectral reflectances of the target. When this ratio normalization is done, the ratio image can then be used in an absolute mode, within the limits of experimental accuracy, which is still under investigation. Preliminary estimates, based on comparing magnitudes of one ratio (channel 7 divided by channel 5) of ERTS MSS data for a clear August 1972 day and a partly cloudy October 1972 day, over a test site near Atlantic City, Wyoming, are that the dark object subtraction and ratio normalization corrections seem good to within a standard error on the order of 5% to 10%. The standard error produced from atmospheric and solar illumination variations for ERTS channel 5 (0.6 - 0.7μm) for the same two days is on the order of 50% or larger. For both of these estimates, bare ground was used as the reference, so as to minimize ground changes. Thus, preliminary indications are that ratio images from ERTS may be useable in an absolute sense, within a standard error of less than 10% from atmospheric and solar illumination variations. For some applications a 10% standard error in the ratio image may be unacceptable, from an absolute point of view. If, however, ratios from a given scanner are available for which a target has higher ratio values than practically anything else in the scene, this standard error should be acceptable for those particular ratios.

The capability of relating ratios of target reflectances determined from a ratio image to those calculated from laboratory spectral reflectance data of various rocks, minerals, and soils has at least three advantages. Laboratory data can be used to indicate whether a given pair of geological targets can be easily discriminated from one another before the geological remote sensing experiment is even conducted. Secondly, if one rock or mineral has an uncommonly high or low ratio value for one particular pair of channels, compared with other possible back-

ground materials in the area, laboratory data of the target and background materials will indicate this, without requiring the production of all possible ratio images from the multispectral scanner data being processed. Possibly the most important advantage, however, is that it may be possible to produce automatic recognition maps with laboratory data as training sets. This subject will not be discussed here, but is presently under investigation.

For ERTS, reflectance ratios for the six non-redundant ratios possible from MSS data (R_{76}, R_{75}, R_{65}, R_{64}, and R_{54}, where R_{ij} means the i^{th} channel divided by the j^{th} channel) have been calculated for all of the rock, mineral, and soil spectra which span the 0.5 - 1.1μm wavelength region in the NASA Earth Resources Spectral Information System (ERSIS) laboratory data collection [5, 6, 7], installed at the Johnson Spacecraft Center and ERIM. Each R_{ij} ratio for ERTS was divided up into ten range intervals, and each interval was assigned a digit ranging from 0 to 9. A six-digit ERTS MSS ratio code was then used to describe the approximate values of the six spectral ratios possible from ERTS data, which permits rapid inspection of the ratio values expected for different rocks and minerals represented in the data bank. These ratio codes are published for 54 soil types (129 laboratory spectra), 82 minerals (181 spectra), 17 rock types (25 spectra), and 15 types of vegetation (18 spectra) in the latest Type II Progress Report [8] from my ERTS contract. A publication of those codes in the open literature is planned within the next six months. Although the ERTS MSS ratio codes from ERSIS laboratory data should be helpful for ratio scannergrammetry investigations, the ERSIS collection of data lacks many appropriate rock, soil, and mineral spectra that could easily be measured in the laboratory and placed into the proper format, if the funds were available for such a task.

EXAMPLES OF RATIO IMAGES

At this point, it is instructive to review some of the examples of ratio images produced over the past three years. Figure 1 shows a thermal infrared ratio image from an early morning, low altitude (1 km) aircraft flight over Pisgah Crater, in Southern California. These images were produced from the ERIM-NASA M-7 multispectral scanner, with a special Honeywell two-element Hg:Cd:Te thermal infrared detector, which is capable of detecting radiances in two overlapping wavelength regions (channel 1, 8.2 - 10.9μm, and channel 2, 9.4 - 12.1μm) simultaneously, with the same instantaneous field of view. The top two strips are single channel images of thermal channels 1 and 2, whereas the bottom strip is a ratio image of channel 1 divided by channel 2. Note that the single channel images show very little contrast across the scene, owing to small temperature variations, except for the sunward side of Pisgah Crater itself. The ratio, however, shows spectral emittance variations across the scene, which are produced in part by variations in $\%SiO_2$ of the silicate rocks present [1,2]. Here the basaltic lava is brighter in the thermal ratio than the more felsic alluvium and wind-blown sand, which are dark.

Figure 2 shows the same thermal ratio compared with a color aerial photograph over an intermittent stream bed, approximately five miles southeast of Pisgah Crater. Volcanic ash flow outcrops (a rhyolitic tuff) are darker than the surrounding alluvium in the ratio image because the rhyolitic tuff has a higher $\%SiO_2$ than the surrounding alluvium. The aerial photo, taken simultaneously with the scanner data at a 1 km altitude above ground, fails to show these outcrops, because the greatest spectral discrimination between the tuff and alluvium occurs at thermal infrared wavelengths, well beyond the spectral range

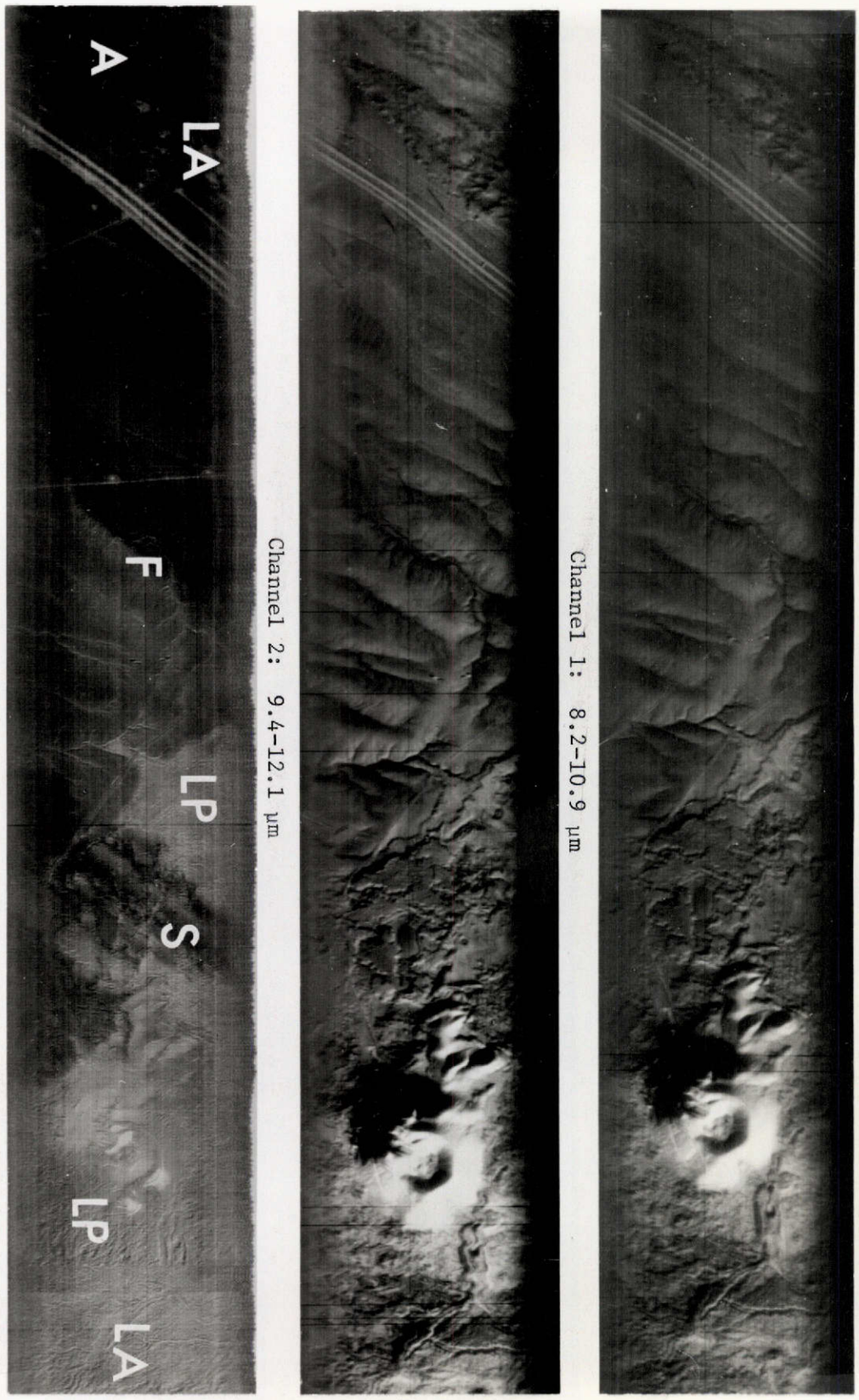

Figure 1. Analog Infrared Images of Flight Line 1, Sec.4, of a North-South Flight over Pisgah Crater. North is toward the left, and the image dimensions are approximately 1.5 km x 6 km. Left to right: alluvium (A); partially covered basaltic lava (LA) of phase 2; highway, fanglomerate, and gravel (F); Pisgah pahoehoe basaltic lava (LP) of phase 3; windblown sand and silt (S); and Pisgah aa basaltic lava (LA) of phases 1 and 2.

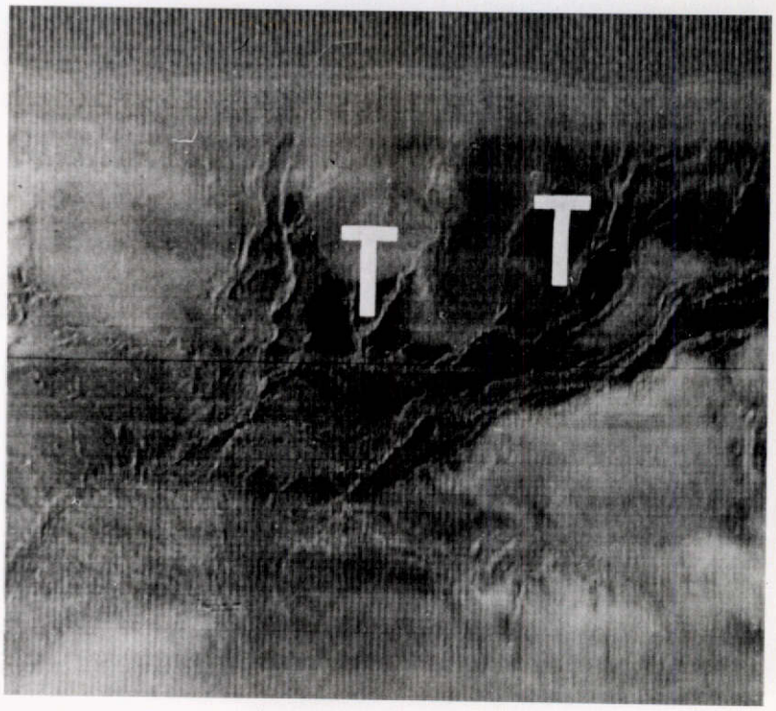

INFRARED RATIO IMAGE

COLOR AERIAL PHOTO

Figure 2. Comparison of Thermal Infrared Ratio Image with an Aerial Photo for a Rhyolitic Tuff (Dark on Ratio Image) Associated with Malachite, near Pisgah Crater, California. North is toward the top and the images are approximately 1.5 km on a side.

of photographic film. In this particular case, malachite (an ore of copper) was associated with the volcanic tuff, but in insufficient quantity to be economical.

The thermal infrared region between 8 and 14μm contains the best spectral information for discriminating among silicate rocks, but multiple channels in that wavelength region are required to take advantage of it. Unfortunately, there is no satellite that has been launched or, to my knowledge, been definitely planned that has a multiple thermal infrared channel capability except for Nimbus E, which was short-lived with regard to its two-channel infrared scanner. It is important for geologic remote sensing, however, that multiple thermal channels be included in some earth resources satellite(s) in the future.

The visible and reflective infrared wavelength regions between 0.4 and 2.5μm contain useful geological information also, but of a different nature. The reflectance of rocks and minerals in this wavelength region are dominated by electronic transitions in ferric (Fe^{+3}), ferrous (Fe^{+2}), copper (Cu^{+2}), and hydroxyl (OH^{-1}) ions and the molecular overtone bands of carbonates and sulfates. The first example [9,4] of a ratio image in these wavelength regions was a reflective infrared to visible green ratio of the same flight line over Pisgah Crater covered by Figure 1. Figure 3 shows the single channel images of a 0.50 - 0.52μm channel and a 0.74 - 0.85μm channel at top and middle, with the ratio image of the two at the bottom. Three eruptive phases of basaltic lava which flowed from Pisgah Crater in the late Pleistocene or early Recent epochs appear in the right half of these images. The lighter-toned region to the right of Pisgah Crater in the ratio image is phase 3 (youngest) lava. Whereas the phase 3 lava in the ratio image is distinct from phase 1 and 2 lava surrounding it, this distinction is not apparent in the single channel images. Sparse chemical data from these flows indicate that this brighter appearance of phase 3 lava in the ratio image, which agrees [4] with laboratory spectra of rock samples from the area, may be caused by the presence of larger amounts of hematite in the youngest lava.

Other examples of ratio imagery can be taken from data collected by ERIM in May of 1972 over a region in the Black Hills of South Dakota for the U. S. Bureau of Mines. Figure 4 shows three ratio images of a flight line over Lead, South Dakota, where the Homestake gold mine is located. In these ratio images, a 0.62 - 0.70μm channel was the common denominator, and the numerator channels were 0.67 - 0.94μm, 1.0 - 1.4μm, and 2.0 - 2.6μm, respectively, from top to bottom in Figure 4. In the top ratio image, called R_{32}, there is a marked contrast between vegetative (bright) and non-vegetative (dark) targets. This R_{32} ratio has proved quite useful for detecting rock outcrops of all kinds in heavily vegetated regions. Even lichen-covered quartzites were easily distinguished from vegetative types of all kinds in this ratio image. This should particularly be useful in Alaska and Canada for locating exposed rock and soil outcrops. The 1.0 - 1.4μm channel divided by the 0.62 - 0.70μm channel (R_{42} ratio) shows the conifers (primarily Ponderosa pine in this region) as dark and vigorous grass as bright, whereas both conifers and grass are bright in the R_{32} ratio image. The bottom ratio image in figure 4, 2.0 - 2.6μm divided by 0.62 - 0.70μm (R_{62}), shows good contrast between the slate, phyllite, and schist of the Cut (to the left of the city) north of Lead and most other targets in the scene. The similarly composed circular mine dump on the other side of Lead and the Maitland tailings (seen at the upper left of the bottom ratio image) also appear darker than most other targets in the scene.

Channel 5 (0.50-0.52 μm)

Channel 7 (0.74-0.85 μm)

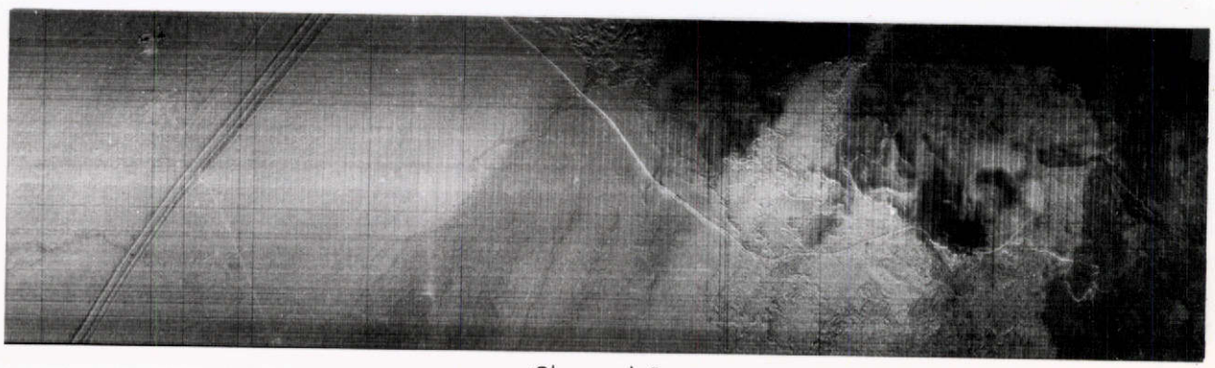

Ratio: $\frac{\text{Channel 5}}{\text{Channel 7}} = R_{57}$

Figure 3. Analog Visible and Reflective Infrared Images of Flight Line 1, Sec.A over Pisgah Crater, California. North is to the left and the images are approximately 1.5 km wide and 6 km long.

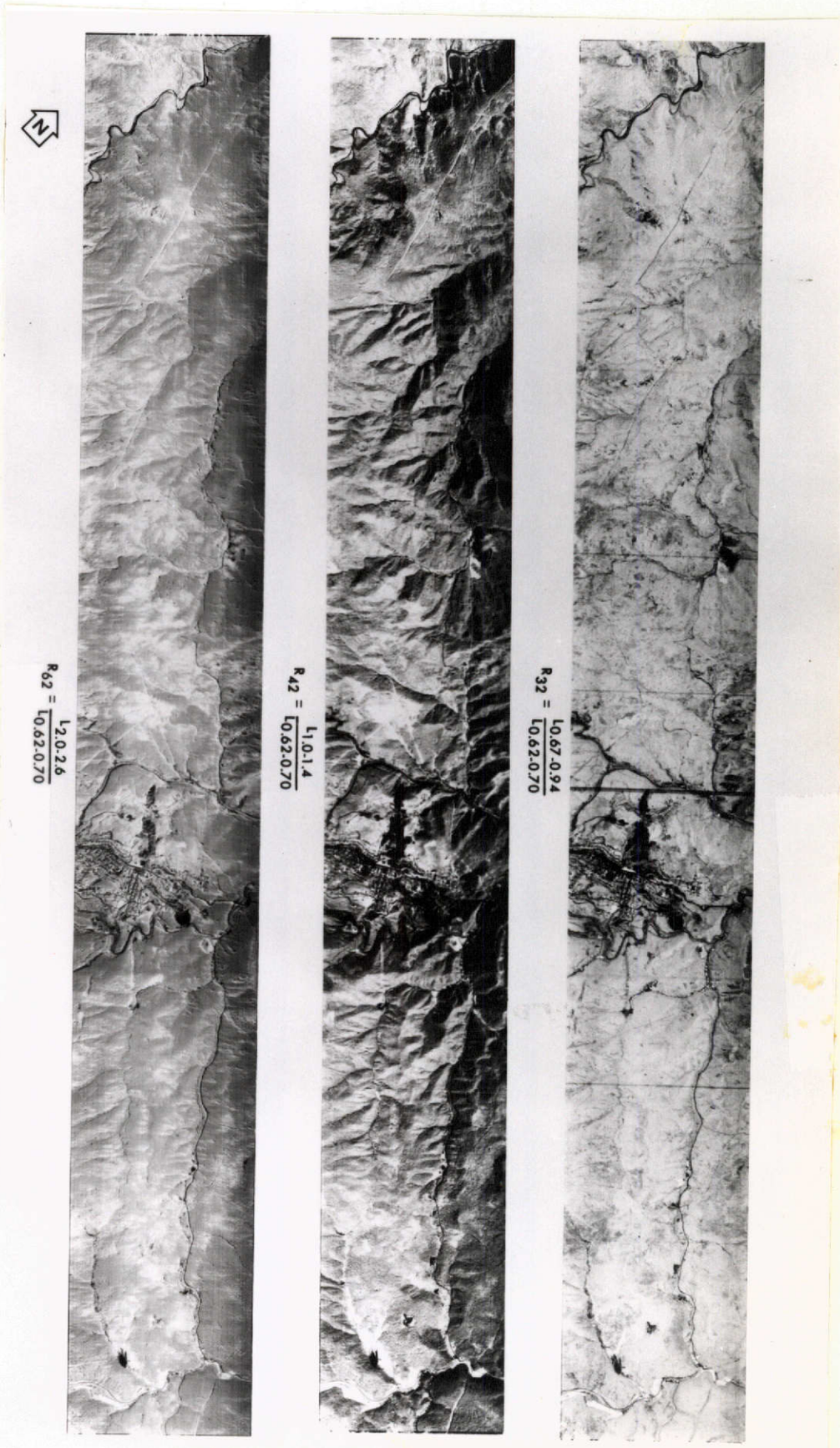

Figure 4. Analog Images of Ratios R_{32}, R_{42}, and R_{62} for Flight Line 2A near Lead, South Dakota. The dimensions of each image are approximately 3 km wide and 36 km long.

For comparison with aerial photography, Figure 5 shows a mosaic of four aerial photos (taken at an approximate altitude of 1.5 km in mid-morning, simultaneously with the scanner data) showing the town of Lead on a different scale. Figure 6 shows a blow-up of the top R_{32} ratio image of Figure 4 for the same region at approximately the same scale as the aerial photomosaic. The contrast between vegetative and non-vegetative targets is much more pronounced in the ratio image. Further, the mosaicing of the aerial photos is not necessary with the scanner imagery. With blow-ups of this R_{32} ratio image, it is possible to detect roadcuts on the order of 3 m in horizontal extent, which was not possible with the air photos.

In all, six ratio images were made from the Black Hills data. Besides the ones shown, images were also made of channels 1.0 - 1.4μm divided by 1.5 - 1.8μm (R_{45}), 2.0 - 2.6μm divided by 1.5 - 1.8μm (R_{65}) and 2.0 - 2.6μm divided by 0.50 - 0.54μm (R_{41}). Table 1 shows the channel number and ratio designations for the Black Hills data. [Note: Channels 1 and 2 here are different from the thermal channels 1 and 2 described earlier.] A gray scale was produced for each ratio image, which relates film density to ratio voltage. As a test to determine what targets in these ratio images could be discriminated, several areas of known rock outcrops and vegetative types were selected, and their ratio voltages were determined by comparing film densities from these areas with gray scales of the respective ratio images. Table 2 shows the resulting ranges of ratio voltages for each ratio and each target. Except for the all non-vegetation target, which encompasses targets 6 through 10, the targets shown in this table are unique from one another in one or more ratios. Figure 7 is a schematic diagram summarizing the targets that could be separated from one another in this data set. When these ratio voltages are reduced to reflectance ratios by normalizing to a known point in the scene, a table similar to Table 2 can be made that is absolute, not relative.

One could locate a point of interest in the scene and determine its ratio voltages by comparing its film density on each of the six ratio images with the respective gray scales. Upon consulting Table 2, one could then say which target group in this table the point of interest belonged to, if any. This is what I would call relative ratio scannergrammetry. If, however, the ratio voltages were converted to reflectance ratios, the point of interest could be compared not only to the targets in Table 2, but also to targets for which laboratory spectra were available in the data bank. The latter I would call absolute ratio scannergrammetry.

The most recent use of ratio images for geological remote sensing is with ERTS data. Figures 8, 9, and 10 show single channel images of ERTS MSS channels 4 (0.5 - 0.6μm), 5 (0.6 - 0.7μm), and 7 (0.8 - 1.1μm), respectively, as produced by ERIM's SPARC analog computer from ERTS computer-compatible tapes, for a small portion of ERTS frame E-1013-17294, 5 August 1972, collected over the U.S. Steel iron mine near Atlantic City, Wyoming. (Note: The channel numbers of the ERTS MSS scanner should not be confused with the aircraft scanner channels defined above.) As an example of how laboratory data can be used to interpret ratio images, the cases of magnetite and hematite (two iron oxides) will be presented. The ERTS MSS ratio code [9] for a magnetite sample from Ishpeming, Michigan is 200006, and for a hematite sample from Irontown, Minnesota is 546459. The ratio codes represent the ratios calculated from ERTS data in order from left to right of R_{76}, R_{75}, R_{74}, R_{65}, R_{64}, R_{54}. The R_{74} ratio code digit for magnetite is 0, meaning that it should be darker in an R_{74} ratio image than approximately 90% of the materials represented in the laboratory data bank described earlier. Hematite has a ratio code digit of 6 for R_{74},

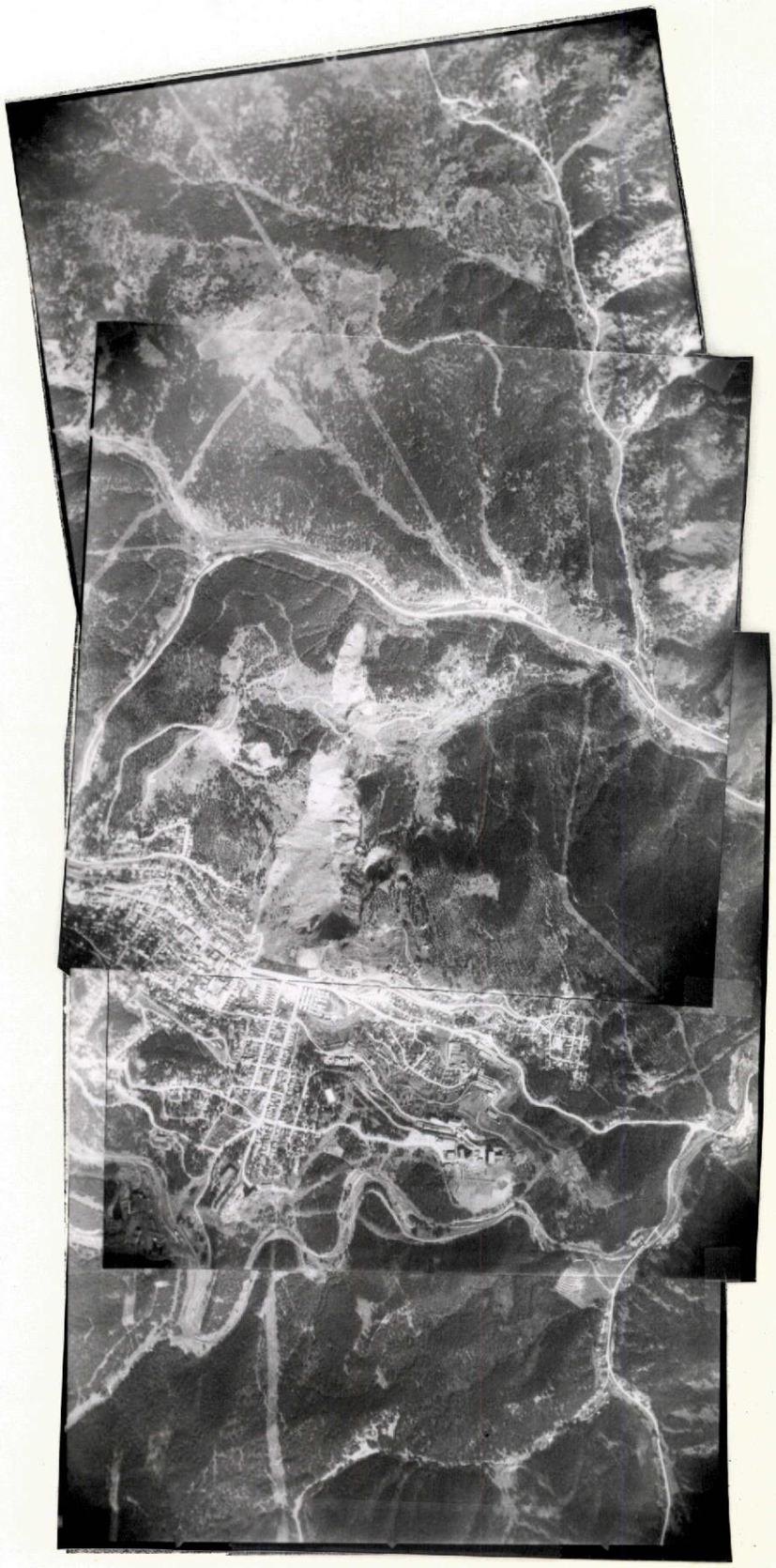

Figure 5. Photo-Mosaic of Aerial Photos Showing the Town of Lead, South Dakota. North is toward the upper right corner and the mosaic represents an area approximately 1.8 km wide and 3.8 km long.

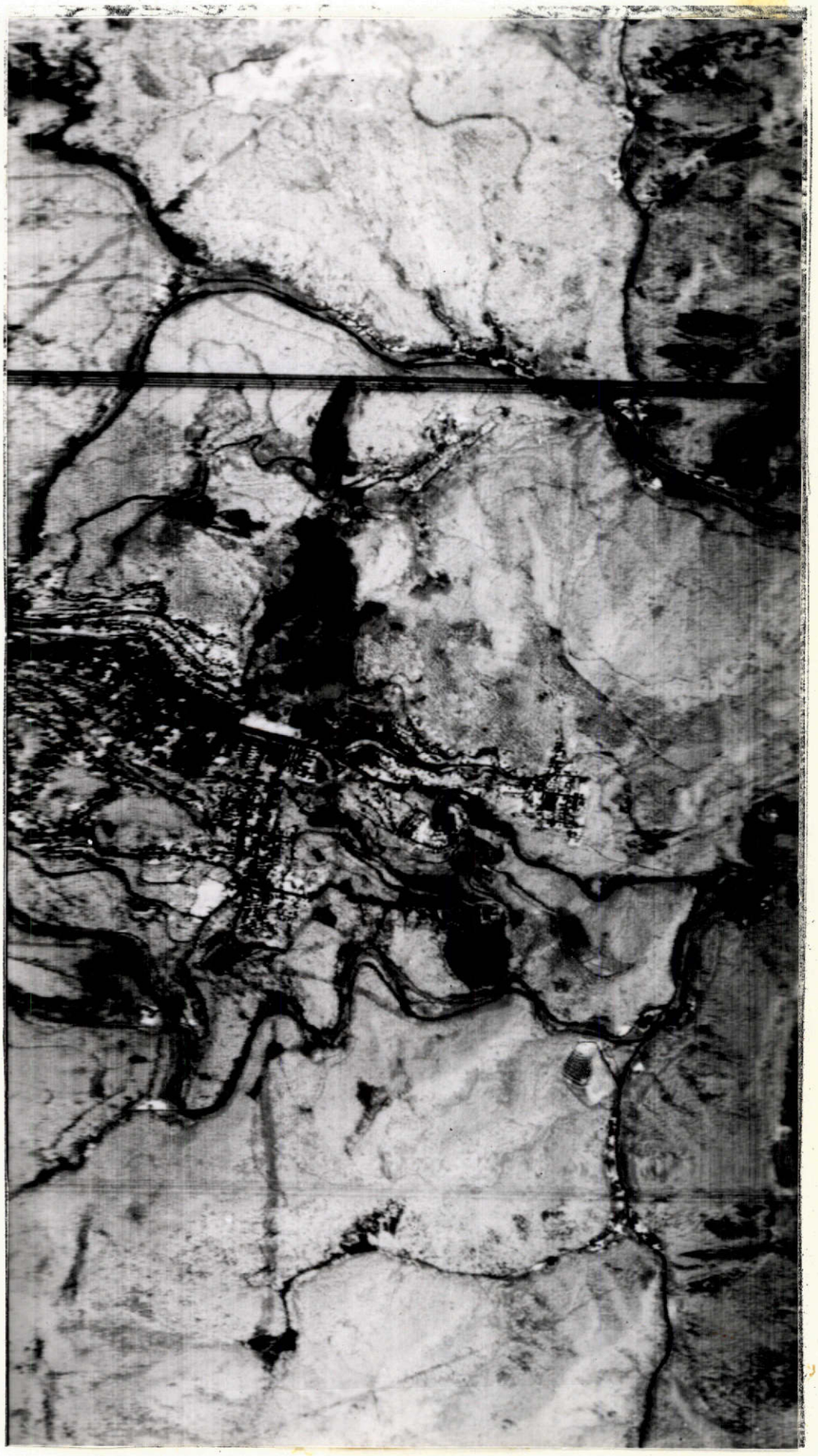

Figure 6. An Enlarged Segment of the $R_{32} \frac{L_{.67-.94}}{L_{.62-.70}}$ ratio image of Lead, South Dakota. North is toward the upper right corner, and the dimensions of the image are approximately 3 km wide and 4 km long.

TABLE 1

List of Spectral Channels and Ratios Used with the Black Hills, S. Dakota Data

Single Channel No.	Wavelength Region (um)	Ratios Including that Channel
1	.50-.54	R_{41}
2	.62-.70	R_{32}, R_{42}, R_{62}
3	.67-.94	R_{32}
4	1.0-1.4	R_{41}, R_{42}, R_{45}
5	1.5-1.8	R_{45}, R_{65}
6	2.0-2.6	R_{62}, R_{65}

TABLE 2

Ratio Ranges of Black Hills Targets

Target No.	Target Name	Ratio Voltage Limits (Volts)						No. of Test Areas
		R_{32}	R_{42}	R_{62}	R_{45}	R_{65}	R_{41}	
1	Vigorous Range Grass	6.6-7.0	4.9-5.3	3.7-4.3	4.1-4.7	2.9-3.5	5.3-5.5	5
2	Dormant and Low Vegetation	2.2-3.4	2.0-3.0	2.4-2.8	2.3-3.1	3.5-4.3	3.5-4.3	7
3	Conifer Trees	4.3-5.9	2.7-3.7	2.6-3.6	3.5-4.5	2.7-3.5	3.6-4.4	3
4	Deciduous Trees	3.0-4.2	2.6-3.6	2.9-3.9	2.3-3.1	3.4-4.2	3.7-4.5	1
5	All Non-Vegetation	0.6-2.2	-	-	-	-	-	-
6	Water	0.6-2.2	0.2-0.8	0.5-2.5	1.4-2.8	0.8-3.4	0.9-2.3	4
7	Quartzite	0.6-2.2	0.4-2.0	2.4-2.8	1.3-2.1	3.7-4.9	0.7-1.9	5
8	Slate, Phyllite, Schist	0.6-1.4	0.5-1.3	0.4-1.4	1.5-2.7	3.7-5.5	0.8-3.0	5
9	Igneous Intrusives (Rhyolite, Quartz Latite, & Phonolite)	0.7-1.3	1.0-1.2	2.0-3.0	1.3-1.9	4.7-5.5	2.2-2.6	7
10	Deadwood Sandstone	0.6-2.2	1.7-1.8	2.2-2.7	2.0-2.5	4.3-5.5	3.0-3.2	2

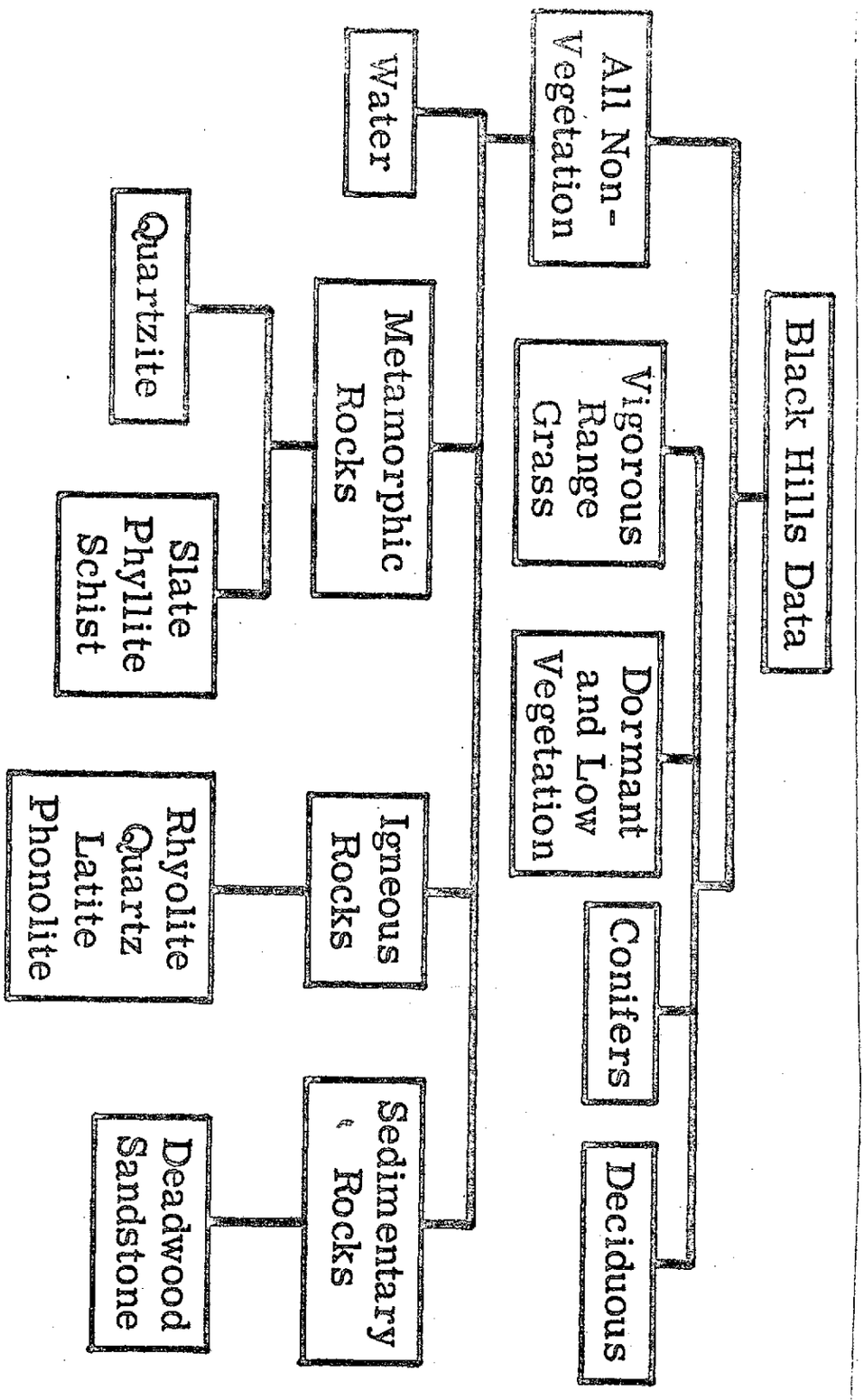

Figure 7. Target Categories for Black Hills, South Dakota, Data Set

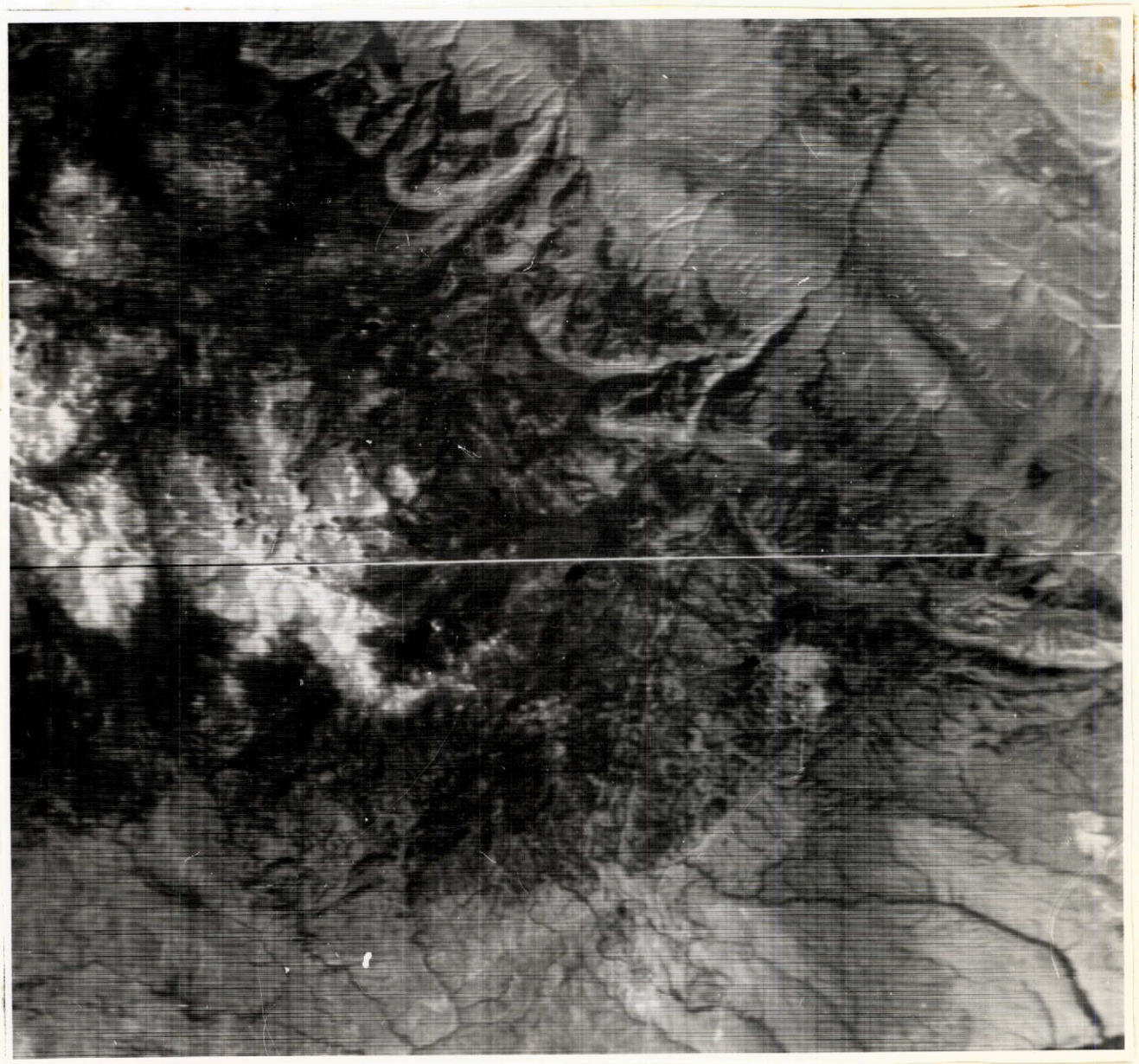

Figure 8. Single channel image of ERTS MSS channel 4 (0.5-0.6μm) for a region near Atlantic City, Wyoming. North is toward the top and the image dimensions are approximately 41 x 46 km.

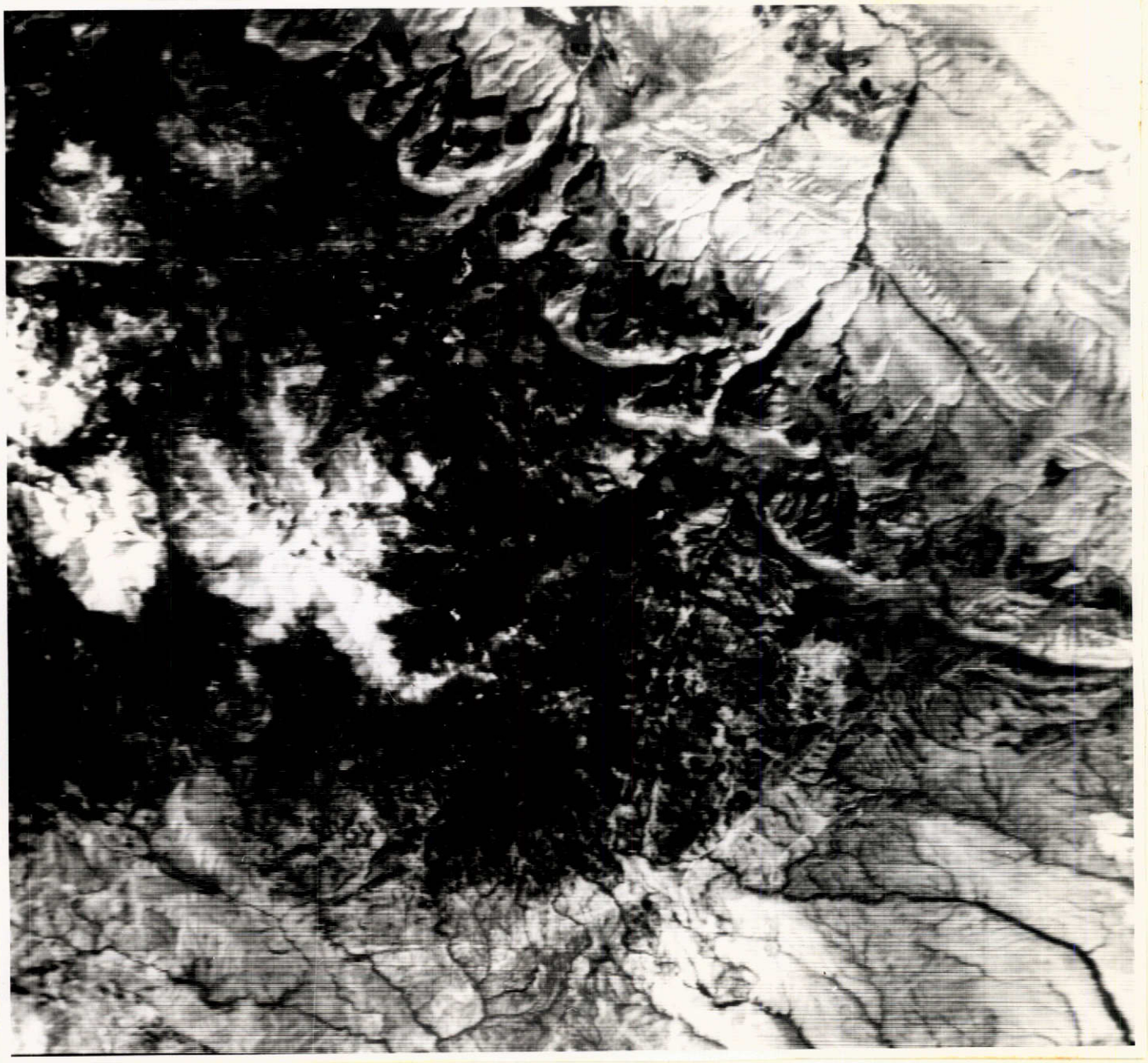

Figure 9. Single channel image of ERTS MSS channel 5 (0.6-0.7μm) for a region near Atlantic City, Wyoming. North is toward the top and the image dimensions are approximately 41 x 46 km.

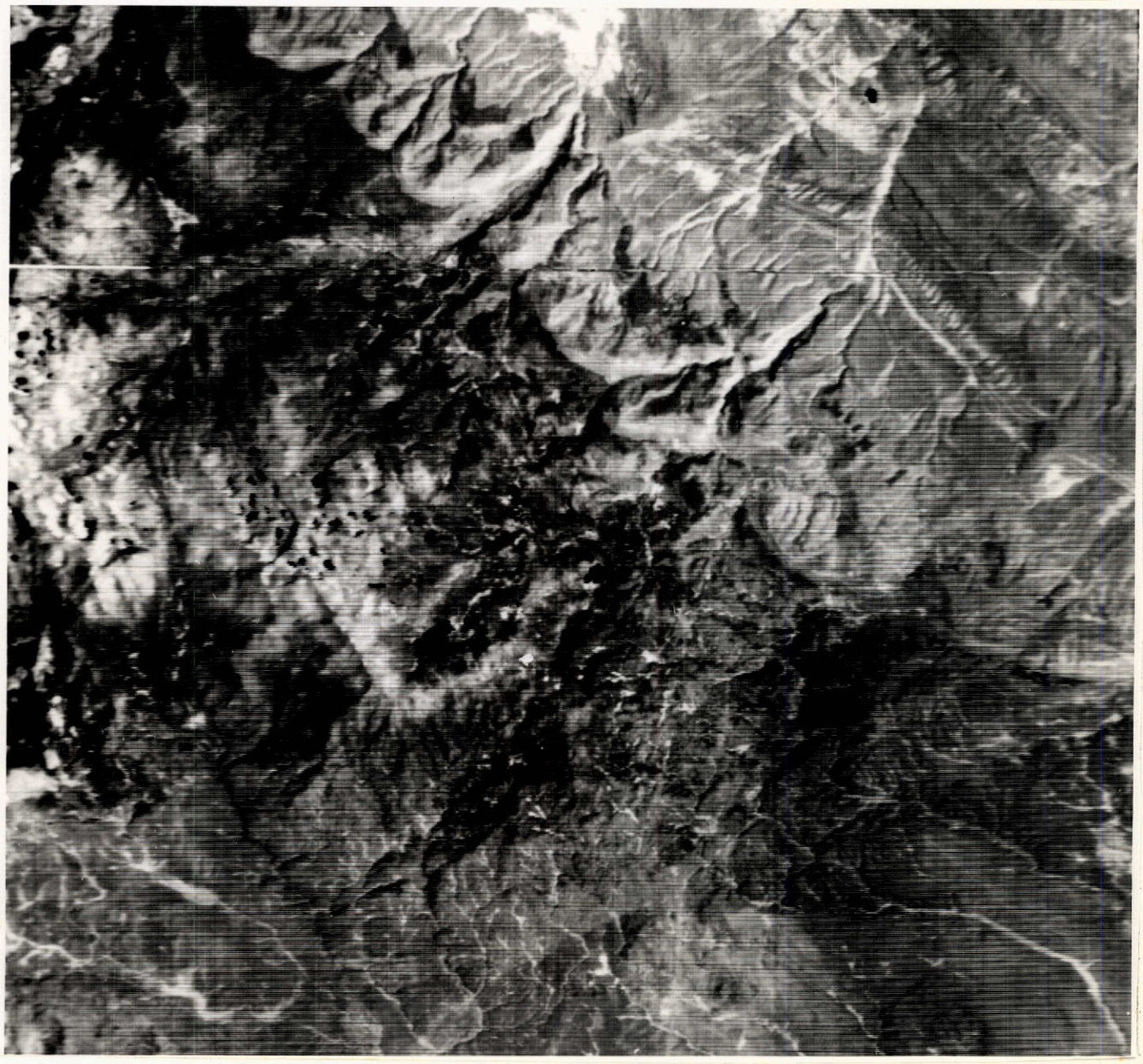

Figure 10. Single channel image of ERTS MSS channel 7 (0.8-1.1μm) for a region near Atlantic City, Wyoming. North is toward the top and the image dimensions are approximately 41 x 46 km.

indicating that it should be brighter than approximately 60% of the materials in the laboratory data bank. Figure 11 shows that the data bank must be fairly representative of the materials in this scene, because magnetite in the iron mine in the lower right portion of the R_{74} ratio image is darker than everything except water, and the hematitic Triassic formations in the upper right corner appear medium-bright in the R_{74} image. The R_{54} ratio code digit for magnetite is 6, whereas it is 9 for hematite. Therefore, the magnetite should appear medium-bright, and hematite should be brighter than about 90% of the materials represented in the laboratory data bank. Figure 12, an R_{54} ratio image, shows that the iron mine is medium-toned, and the Triassic red beds are the brightest objects in the scene. In fact, the R_{54} ratio image of the whole ERTS frame, not shown here, delineates well all of the hematitic Triassic formations that have been mapped in the area covered by the entire ERTS frame. The ratio codes for limonite (a field term for hematite or goethite which contains relatively large amounts of H_2O) samples indicate the limonite will be similar to hematite in these two ratio images, but will be much darker than hematite (in fact, darker than almost anything else) in an R_{76} ratio image. No large limonite exposures have been found as yet in the test area, however. The ability to separate these iron oxides may be useful for mineralogical exploration, particularly copper exploration.

As might be expected, not many targets are unique with only four channels of ERTS data. In progress is an effort to define from laboratory data which geological targets will be confused with one another, within the limits of the laboratory data bank as it now stands.

CONCLUSIONS

A description of ratio images and several examples of their application to geological remote sensing problems have been described. Ratio scannergrammetry, defined for this paper as the treatment of scanner ratio images with photogrammetric techniques, offers the user a means of determing (from laboratory data) what a given material will look like in a particular ratio image, even before the data are collected. When the laboratory data bank is expanded to include more rock and mineral samples, it may eventually be possible to interpret ratio images over completely unknown terrain with acceptable accuracy.

Geological applications for the ratio techniques discussed above may include the following:

1. Exploration for construction materials (sand and gravel)
2. Surveying of beaches (quartz versus calcite sands and mapping of sand dunes)
3. Exploration for ophiolites
4. Mapping of volcanic ash flows
5. Mineralogical exploration (especially for ores related to iron oxides)
6. Stratigraphic mapping (now being attempted with ERTS data)
7. Soil mapping
8. Assessment of the extent of known mineralogical resources
9. Finding lichen-covered rock outcrops in vegetated terrain
10. Monitoring open pit mining operations

The thermal infrared ratio is best for the first four applications, and visible-reflective infrared ratios are best for the last two. A combination of all ratios would be desirable for the other applications.

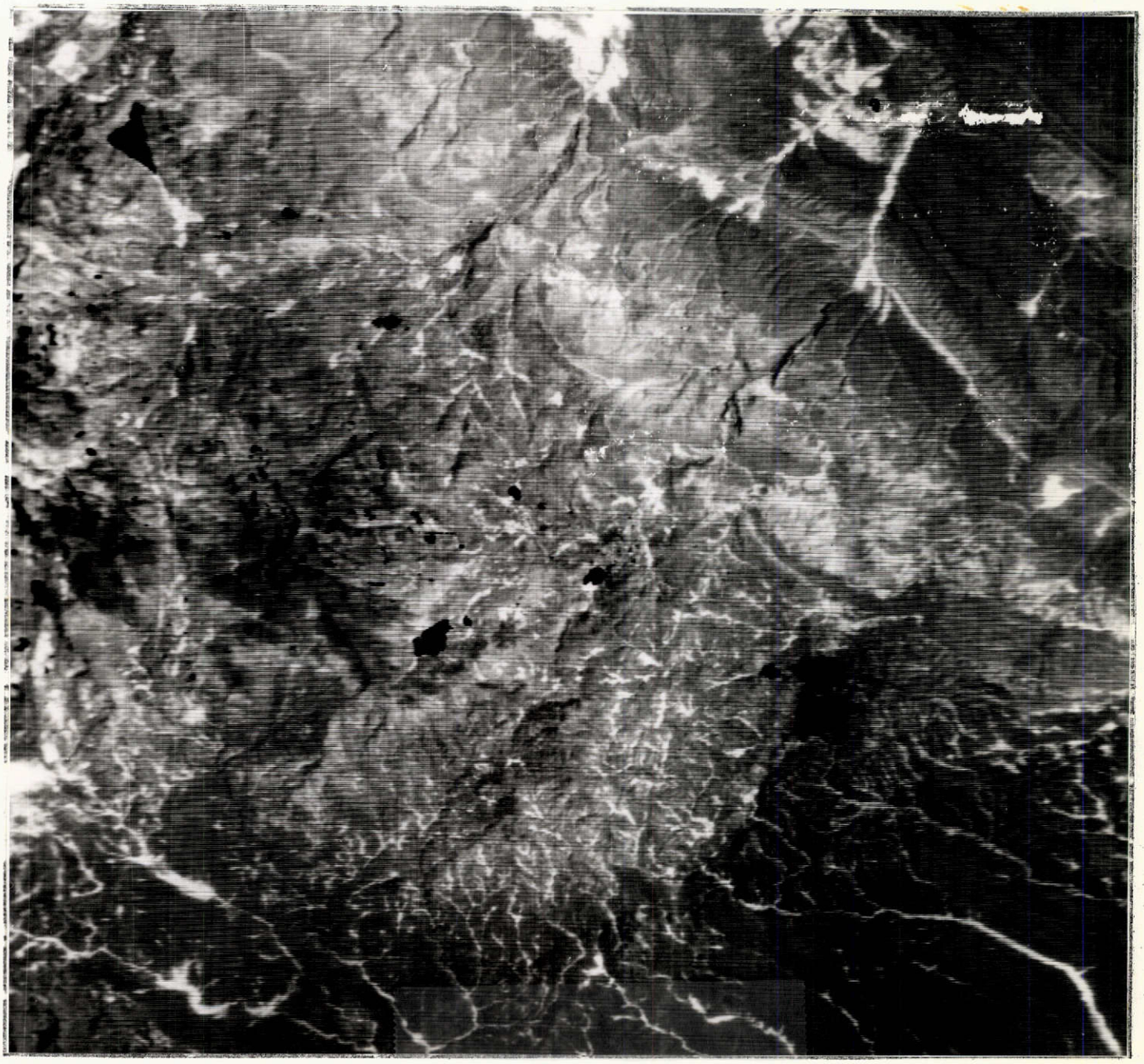

Figure 11. ERTS $R_{74} \frac{L_{0.8-1.1}}{L_{0.5-0.6}}$ ratio image for a region near Atlantic City, Wyoming. Iron mine at lower right is dark and Triassic formations at upper right (trending Northwest) are medium-bright. North is toward the top and the image dimensions are approximately 41 x 46 km.

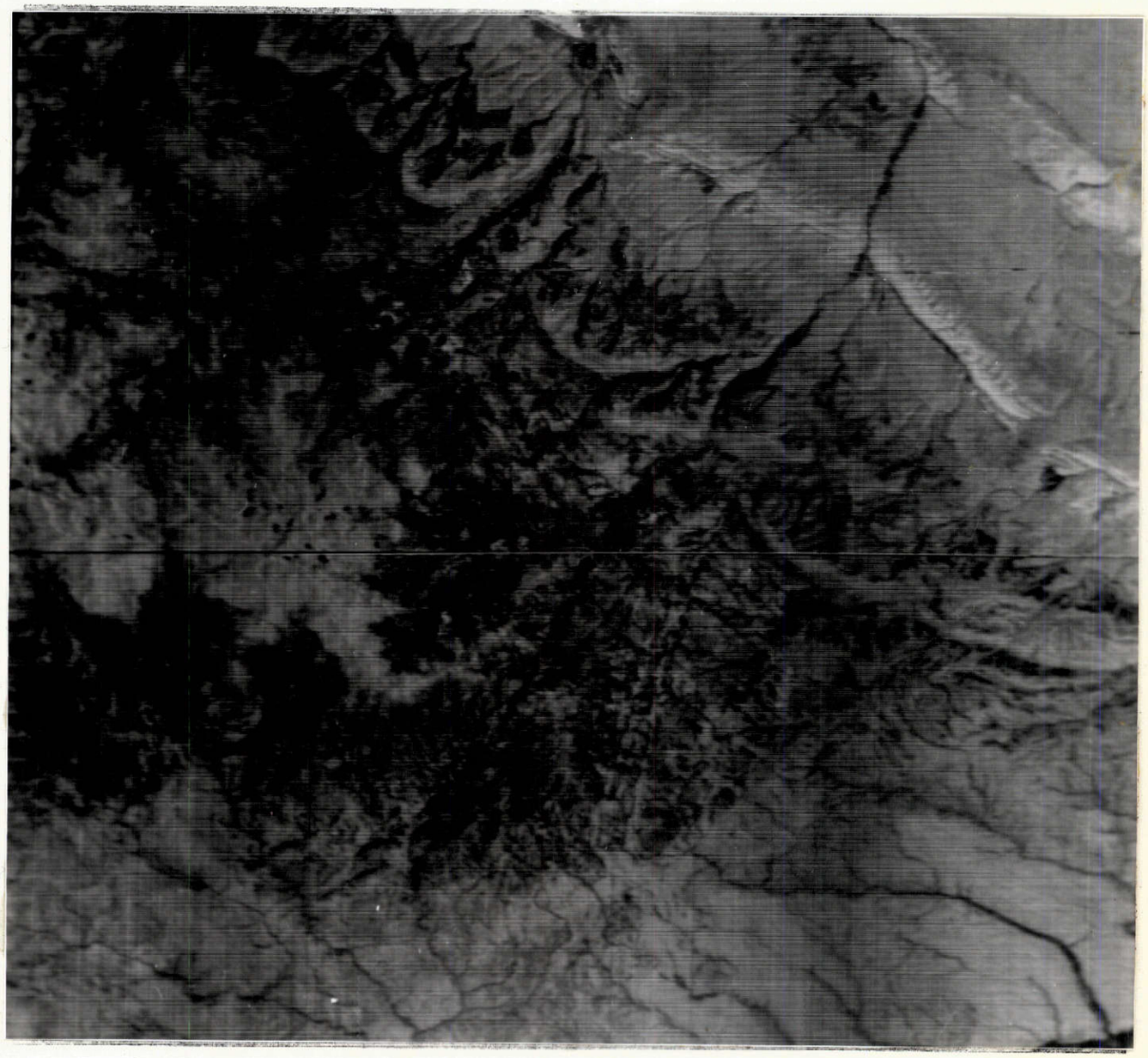

Figure 12. ERTS $R_{54} \frac{L_{0.6-0.7}}{L_{0.5-0.6}}$ ratio image for a region near Atlantic City, Wyoming. Iron mine at lower right is medium-toned and Triassic formations at upper right (trending Northwest) are brightest in the scene. North is toward the top and the image dimensions are approximately 41 x 46 km.

Yet to be completed are expansion and improvement of the data base of laboratory spectra; determination of the experimental accuracy of the ratio images; the combination of visible, reflective infrared, and thermal infrared ratio images with single data sets; and the attempted use of scanner ratios and laboratory data to define a method and an operational system for producing completely automatic recognition maps, with computer-stored ratio codes for identifying target materials.

ACKNOWLEDGEMENTS

My thanks to Ben Drake for the ratio voltage determinations in Table 2 and able assistance with ground truth operations, to Bette Salmon and William Pillars for their valuable assistance with all facets of the work in our ERTS contract, and to Dr. Jon Erickson for his constructive comments. This work was supported by NASA contracts NAS-9-9784 and NAS-5-21783 and the Advanced Research Projects Agency of the Department of Defense, as monitored by the U.S. Bureau of Mines under Contract No. H0210041.

REFERENCES

1. "Rock Type Discrimination from Ratioed Infrared Scanner Images of Pisgah Crater, California," R. K. Vincent and F. Thomson, Science, Vol.175, pp.986-988, 1972.

2. "Spectral Compositional Imaging of Silicate Rocks," R. K. Vincent and F. Thomson, J.of Geophysical Research, Vol.77, pp.2465-2471, 1972.

3. "Recognition of Exposed Quartz Sand and Sandstone by Two-Channel Infrared Imagery," R. K. Vincent, F. Thomson and K. Watson, J. of Geophysical Research, Vol.77, pp.2473-2477, 1972.

4. "An ERTS Multispectral Scanner Experiment for Mapping Iron Compounds," R. K. Vincent, Proceedings of the 8th International Symposium on Remote Sensing of Environment, Ann Arbor, Michigan, pp.1239-1247, 1972.

5. "The NASA Earth Resources Spectral Information System: A Compilation," V. Leeman, D.Earing, R. Vincent and S. Ladd, NASA Rept. NASA CR-31650-24-T, NASA Contract NAS9-9784, University of Michigan, Ann Arbor, Michigan, 1971.

6. "The NASA Earth Resources Spectral Information System: A Compilation, First Supplement," V. Leeman, NASA Report NASA CR-WRL 31650-69-T, NASA Contract NAS9-9784, University of Michigan, Ann Arbor, Michigan, 1972.

7. "The NASA Earth Resources Spectral Information System: A Compilation - Second Supplement," R. K. Vincent, NASA Rept. NASA CR-ERIM 31650-156-T, NASA Contract NAS9-9784, Environmental Research Inst. of Michigan, 1973.

8. "ERIM Progress Report on Use of ERTS-1 Data, Summary Report on Ten Tasks, Type II Progress Report, for Period 1 Jan.-30 June, 1973," F. Thomson, et.al., ERIM, NASA Contract NAS5-21783, Rept. No. 193300-16-P, 1973.

9. "Experimental Methods for Geological Remote Sensing," R. K. Vincent, 4th Annual Earth Resources Program Review Proceedings, NASA Manned Spacecraft Center, Houston, Texas, V.II, p.33-1, January 1972.